Prediction and final temporal errors are used for trial-to-trial motor corrections

Joan López-Moliner[1], Cécile Vullings[2], Laurent Madelain[2], Robert J. van Beers[3]

[1]Vision and Control of Action (VISCA) Group, Department of Cognition, Development and Psychology of Education, Institut de Neurociències, Universitat de Barcelona, Passeig de la Vall d'Hebron 171 08035 Barcelona, Catalonia, Spain

[2]CNRS, CHU Lille, UMR 9193, SCALab Sciences Cognitives et Sciences Affectives, Université de Lille, Lille, France

[3]Department of Human Movement Sciences, Vrije Universiteit Amsterdam, Amsterdam, The Netherlands and Radboud University, Donders Institute for Brain, Cognition and Behaviour, Nijmegen, The Netherlands

Abstract

Correction on the basis of previous errors is paramount to sensorimotor learning. While corrections of spatial errors have been studied extensively, little is known about corrections of previous temporal errors. We tackled this problem in different conditions involving arm movements (AM), saccadic eye movements (SM) or button presses (BP). The task was to intercept a moving target at a designated zone (i. e. no spatial error) either with the hand sliding a pen on a graphics tablet (AM), a saccade (SM) or a button press (BP) that released a cursor moving ballistically for a fixed time of 330 ms. The dependency of the final temporal error on action onset varied from "low" in AM (due to possible online corrections) to "very high" in the other conditions (i.e. open loop). The lag-1 cross-correlation between action onset and the previous temporal error were close to zero in all conditions suggesting that people minimized temporal variability of the final errors across trials. Interestingly, in conditions SM and BP, action onset did not depend on the previous temporal error. However, this dependency was clearly modulated by the movement time in

the AM condition: faster movements depended less on the previous actual temporal error. An analysis using a Kalman filter confirmed that people in SM, BP and AM involving fast movements used the prediction error (i.e. intended action onset minus actual action onset) for next trial correction rather than the final target error. A closer look at the AM condition revealed that both error signals were used and that the contribution of each signal follows different patterns with movement time: as movement progresses the reliance on the prediction error decreases non-linearly and that on the final error increases linearly.

Author summary

Many daily life situations (e.g. dodging an approaching object or hitting a moving target) require people to correct planning of future movements on the basis of previous temporal errors. This is paramount to learning motor skills. However the actual temporal error can be difficult to measure or perceive: imagine, for example, a baseball batter that swings and misses a fastball. Here we show that in these kinds of situations people can use an internal error signal to make corrections in the next trial. This signal is based on the discrepancy between the actual action onset and the expected one. The relevance of this error decreases with the movement time of the action in a particular way while the final actual temporal error gains relevance for the next trial with longer motor durations.

Introduction

Timing errors of actions are ubiquitous in daily-life and learning from these errors to improve planning of future movements is of great importance. Suppose you are batting in a baseball game and you just missed a fast ball by 50 ms. Assuming you validly expect another fast ball, how and how much you should you correct for this error in the next movement may depend on different factors. You could use an estimate of this temporal error (between the bat and the ball) and try to react earlier if you were late. However your measurement of this error can be noisy. Since the movement time of your hitting movement can be quite constant you could alternatively rely on correcting the start of the swing relative to some relevant moment (e.g. ball motion onset). In this study, we address on what basis one corrects for temporal errors under different situations of uncertainty about the final temporal error and the possibility of correction during the movement. Correcting on the basis of previous errors is one of the hallmarks of motor learning (1,2) and many studies have addressed how people correct for spatial errors when there is some external perturbation (e.g. with force-fields or distorted visual feedback) (3-7) or in situations without perturbations (8).

It is known that larger uncertainty on the observed spatial error leads to smaller corrections (5,9,10). This is either because one would weight the final sensed error less relative to some internal prediction of the error, as predicted by Bayesian frameworks (11) (see Fig1A), or because the noise added by the movement execution is relatively large compared to the noise in planning that movement (8). The possibility of control while unfolding the action could also affect the relevance of the final temporal error. For instance, in open loop actions or when the movement time is very stable (e.g. the baseball example

67 or in saccadic eye movements) the time of action onset becomes relevant to the final
68 temporal error (i.e. they are highly correlated) and one could weight the final error less and
69 base the corrections on some prediction error between the intended and actual action
70 onset (Fig1A). This can be so especially in fast movements in which predictive components
71 are important. Alternatively, both prediction and final errors can be used in combination to
72 specify the next trial correction. We consider these possibilities in this study.

73 We know that predictions based on forward models (12) are important for correction
74 mechanisms in general. That is, discrepancies between the prediction and some feedback,
75 be it internal or sensed (13), are the key for mainstream computational models of motor
76 learning (14,2) to explain the corrections of saccadic movements (15) or fast arm
77 movements which are too brief to benefit from the final sensory feedback. In particular, in
78 conditions where humans are aware of perturbations, errors based on internal predictions
79 can even override final target spatial errors (16) leading to the distinction between
80 different kinds of errors: aiming errors (i.e. discrepancy between the planned and final
81 positions) and target errors (i.e. target vs final position discrepancy), which are important
82 in motor learning models (17).

83 Here, we resort to a similar distinction: errors based on the discrepancy between internally
84 predicted and sensed action onset (prediction error) and temporal errors based on the
85 experienced sensory feedback at the end of the movement. We expect a different
86 contribution of each error type in the next trial correction depending on how fast the
87 movements are (i.e. prediction error being more relevant in faster movements). We test
88 this hypothesis by using temporal corrections in an interception task.

We will consider the situation in which errors arise when inappropriate motor commands are issued (execution errors) as opposed to errors caused by external changes (18,5). In order to see the extent of the corrections, we exploit the properties of the time series of action onset in arm movements, saccadic eye movements and button-presses to study how people correct when the initial prediction error at action onset (see Fig1A) contributes differently to the final sensory temporal error with respect to a moving target in the different conditions. In the button press condition, a keypress released a fixed movement cursor to intercept the target. In this condition and in the eye movements condition the prediction error is highly correlated with the final temporal error. However, the former error can be perceived with high perceptual uncertainty in the eye movements condition due to the variability of saccadic reaction time and the temporal and spatial distortions at the time of saccades starting about 50 ms before saccade onset and up to 50ms after saccade offset, a phenomenon often termed saccadic suppression (19,20). Finally, arm movements with different movement times will enable us to determine whether the relative contribution of either type of error depends on the movement time. A model based on a Kalman filter will be used to obtain an estimate of the predicted action onset and therefore, the prediction error. We show that both prediction error relative to action onset and final temporal error relative to the target can be used in combination for trial-to-trial corrections. The contribution of each error signal follows a specific time course since action onset.

Methods

Arm movement experiment

Participants

15 subjects (age range 22-33, 11 males) participated in the experiment. Twelve of them were right-handed and three were left-handed as by self-report. All of them had normal or corrected-to-normal vision, and none had evident motor abnormalities. All subjects gave written informed consent. The study was approved by the local research ethics committee.

Apparatus

Participants sat in front of a graphics tablet (Calcomp DrawingTablet III 24240) that recorded movements of a hand-held stylus. Stimuli were projected from above by a Mitsubishi SD220U ceiling projector onto a horizontal back-projection screen positioned 40 cm above the tablet. Images were projected at a frame rate of 72 Hz and a resolution of 1024 by 768 pixels (60 x 34 cm). A half-silvered mirror midway between the back-projection screen and the tablet reflected the images shown on the visual display giving participants the illusion that the display was in the same plane as the tablet. Lights between the mirror and the tablet allowed subjects to see the stylus in their hand. Virtual moving targets were white dots on a black background (shown red on white in Fig 1A). A custom program written in C and based on OpenGL controlled the presentation of the stimuli and registered the position of the stylus at 125 Hz. The software ran on a Macintosh Pro 2.6 GHz Quad-Core computer. The set-up was calibrated by aligning the position of the stylus

with dots appearing on the screen, enabling us to present visual stimuli at any desired position of the tablet.

Procedure

To start each trial, subjects had to move the stylus to the home position (grey dot in Fig 1B). After a random period between 0.8 and 1.2 seconds, a moving target that consisted of a white dot of 1.2 cm diameter appeared moving rightwards (or leftwards for left-handed subjects). Targets could move at one of three possible constant speeds (20, 25 or 30 cm/s), interleaved across the session. The target moved towards two vertical lines of 2 cm height and separated by 1.2 cm. The space between the lines was aligned with the home position (Fig 1B). Subjects had to hit the target (i.e. passing through it) at the moment the target was between the two vertical lines. Because we instructed participants to hit the target in the interception zone, we only had temporal errors associated to responses, except for the trials in which subjects missed the zone (less than 2%). The starting position of the target was determined by the initial time to contact (i.e. time for the target to reach the interception zone) value, which was 0.8 s for all target speeds. Auditory feedback was provided (100ms beep at 1000Hz) whenever the absolute temporal error between the hand and the target was shorter than 20 ms when the hand crossed the target's path between the two lines. Each subject completed 360 trials.

Data analysis

The individual position data time series were digitally low-pass filtered with a Butterworth filter (order 4, cut-off frequency of 8 Hz) for further analysis. Hand tangential velocity was

computed from the filtered positional data by three-point central difference calculation. For each trial, we then computed the time of arm movement onset, the peak velocity, the movement time (elapsed time from the hand movement onset until the hand crossed the target's path), and the temporal error with respect to the target. Movement onset was computed offline by using the A algorithm reported in (21) on the tangential velocity of the hand.

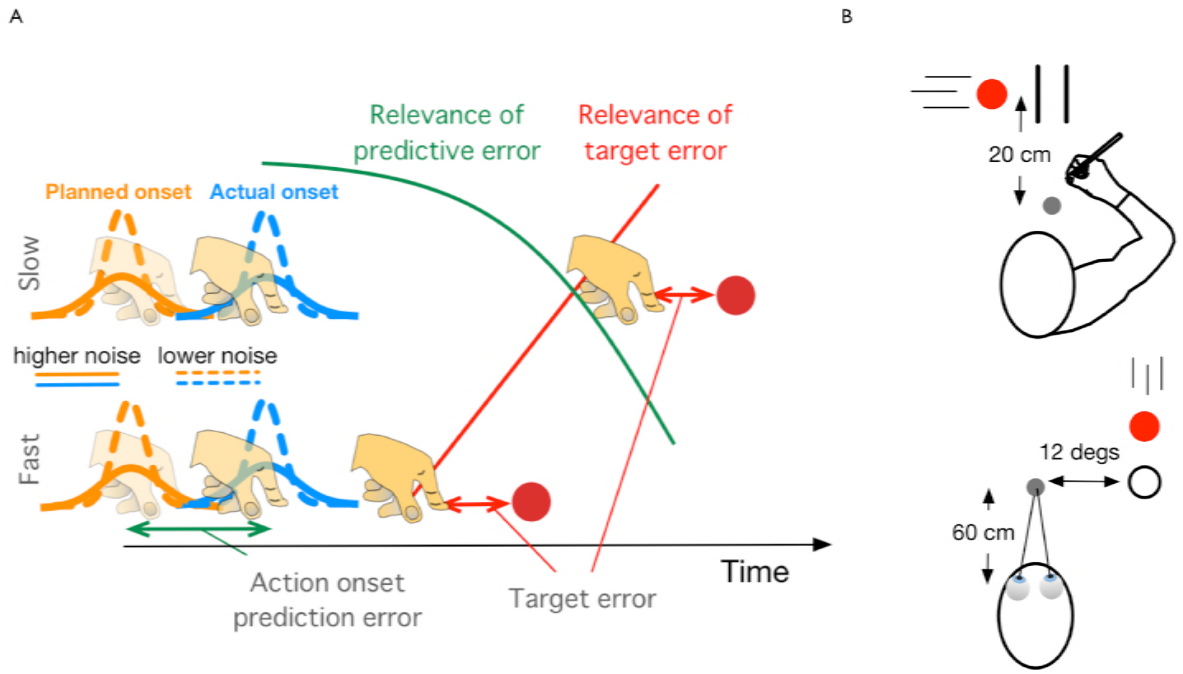

Fig 1. (A) Action onset and its reliability to predict the relevant task variable: temporal error with respect to the moving target. The uncertainty in determining the planning of the action onset (hidden variable) is illustrated by the orange Gaussians, while the execution (or measurement) noise is denoted by the blue Gaussians centered at the actual action onset. Different variability in the planning of action onset or its measurement is denoted by the type of line (dashed: lower noise; solid: higher noise). The prediction error is the difference between the planned (or predicted) and actual action onset. The top row illustrates a slow movement after action onset (longer duration until crossing the target) and the bottom row a

fast movement. One would expect larger corrections when the measurement noise of the actual action onset is lower (blue dashed curves) relative to the planned noise (solid orange curves). The decay of the relevance of the prediction error after action onset is denoted by the green line, while the increasing relevance of the final temporal error for next trial is denoted by the red line. These particular trends are based on the assumption that the quadratic sum of both lines would sum up to one. (B) Illustration of the experimental tasks: arm movements (top) and eye movements (bottom).

Button press experiment

Participants

Eight participants (age range 23-32, 5 males) participated in this experiment. All of them had normal or corrected-to-normal vision, and none had evident motor abnormalities. All subjects were right handed and gave written informed consent. The study was approved by the local research ethics committee.

Apparatus

Stimuli were shown on a Philips CRT-22 inch (Brilliance 202P4) monitor at a frame rate of 120 Hz and a resolution of 1024 by 768 pixels. The viewing distance was about 60cm and the head was free to move. A custom program written in C and based on OpenGL controlled the presentation of the stimuli and registered the time of the button-presses by sampling an ancillary device at 125 Hz. The software was run on a Macintosh Pro 2.6 GHz Quad-Core computer.

Procedure

The stimuli were the same as in the Arm Movement experiment except for the fact that the motion was presented on the fronto-parallel plane. In this experiment subjects had to press a button that initiated the release of a moving cursor from the home position. Subjects had to press the button timely so that the cursor would hit the target when passing between the two vertical lines (interception zone). The movement time of the cursor from the home position to the interception zone was 312 ms and its velocity profile was extracted from an actual arm movement. In this experiment the time of the button-press determined completely the final temporal error. Subjects took the same number of trials and sessions as in the Arm movement experiment.

Eye Movement experiments

Participants

Fifteen participants (age range 18–47, 7 males, including two authors) participated in the experiments. Among them, ten (age range 18–46, 4 males) participated in th first experiment (termed knowledge of results, KR) and twelve (age range 23-47, 5 males) participated in the second one (knowledge of performance, KP). They had normal or corrected-to-normal vision. All participants gave written informed consent. The study was approved by the local research ethics committee.

Apparatus

Stimuli were generated using the Psychophysics Toolbox extensions for Matlab® (22,23) and displayed on a video monitor (Iiyama HM204DT, 100 Hz, 22''). Participants were seated on an adjustable stool in a darkened, quiet room, facing the center of the computer screen at a viewing distance of 60 cm. To minimize measurement errors, the participant's head movements were restrained using a chin and forehead rest, so that the eyes in primary gaze position were directed toward the center of the screen. Viewing was binocular, but only the right eye position was recorded in both the vertical and horizontal axes. Eye movements were measured continuously with an infra-red video-based eye tracking system (Eyelink®, SR Research Ltd., 2000 Hz) and data were transferred, stored, and analyzed via programs written in Matlab®. The fixation point that was used as a home position for the gaze was a 0.4 deg×0.4 deg square presented always on the bottom left quadrant of the screen. The target was a 0.4 deg of diameter disk, and the interception area was a goal box of 0.6 deg of diameter. The interception area was located 12 deg to the right of the home position (see Fig 1B). All stimuli were light grey (16 cd/m^2 luminance) displayed against a dark grey background (1.78 cd/m^2 luminance). Before each experimental session, the eye tracker was calibrated by having the participant fixate a set of thirteen fixed locations distributed across the screen. During the experiment the subject had to look at the center of the screen for a one-point drift check every fifty trials. If there was any gaze drift, the eye tracker was calibrated again.

Procedure

A session consisted of 390 discrete trials lasting between 2 and 2.45 secs. Each trial started with the subject looking at the fixation point for a period randomly varying between 700 and 1100ms. Participants were instructed to make a saccade to intercept the target, that was moving downward towards the interception area, at the time it was within the interception area. Targets moved with a constant velocity of either 20, 25 or 30 deg/s. Target velocities were interleaved across trials in both the KR and KP-interleaved experiments. In the KP-blocked condition, the targets' velocities were presented in three consecutive 130-trial blocks (in a pseudo-random order counterbalanced across participants). The same participants experienced both KP conditions; the order was counterbalanced across subjects. The time to contact the interception area was 600 ms since target onset, and the target starting point was therefore depended on the actual target velocity. The occurrence of a saccade was crudely detected when the online eye velocity successively exceeded a fixed threshold of 74 deg/s. If the offset of an ongoing saccade was detected before the target reached the interception zone the target was extinguished at the next frame, i.e. within the next 10ms (offline measurements revealed that the target disappeared on average 2 ms after the time of the actual saccade offset). If the target center was aligned with the goal box before a saccade was detected we extinguished the target. Therefore, participants never saw the target after it had reached the interception zone. We delivered an auditory feedback (100 ms beep at 1000 Hz) if the eye landed within 3 deg of the interception area with an absolute temporal error smaller than 20 ms. To this end, the actual saccade onset- and offset-time and position were

computed immediately after the saccade using the real-time Eyelink algorithm with a 30 deg/s velocity and 8000 deg/s^2 acceleration thresholds (on average we retrieved these values 12 ms after the end of the saccade). In the first experiment (KR), participants did not receive explicit feedback on their performance other than the auditory one. In the second experiment (KP), the actual temporal error was displayed numerically in milliseconds at the end of each trial (KP). For offline analyses, a human observer validated each saccade manually. Saccades with an amplitude gain smaller than 0.5 or a duration longer than 100 ms were discarded.

Analysis

Testing for the optimality of corrections: autocorrelation analysis

It is known that the serial dependence of consecutive movement errors depends on the amount of trial-by-trial correction (24). If participants are trying to make temporal corrections based on the prediction error we should be able to see a serial dependence of the action onset (T^s) in both simulated and behavioral data that will depend on β, the fraction of correction. Suppose that no corrections are made whatsoever. In this case, we expect that consecutive initiation times will be similar to the previous one. The absence of correction would be revealed by a significant positive lag-1 autocorrelation function (acf(1)) of the action onset under the assumption that planning noise accumulates from trial to trial. On the contrary, if one aims at correcting for the full observed error (β=1) then consecutive movements will tend to be on opposite sides of the average response because one corrects not only for the error in planning but also for the random effects of execution

noise. In both scenarios (β=0 and β=1) there is an unnecessarily large temporal variability due to different causes. If one does not correct, not only will previously committed errors persist but also previous planning errors will accumulate across trials increasing the variability much like when one repeatedly reaches out for static targets. If one does fully correct, the variability due to changes in the planned time will be larger than if smaller corrections were made. In either case the process is not optimal in the sense that the temporal error is more variable than necessary. When corrections are large enough to compensate for random variability but not too large to make the behavior unstable, then the temporal error variance is minimal and the correction fraction is optimal. For such fractions of corrections, acf(1) of the temporal errors will be zero (8). In our case participants can correct by changing the action onset, so we are interested in the cross-correlation function (ccf(1)) between action onset at trial *i* and the relevant target error at trial *i-1*. Note that for the button press condition action onset is perfectly correlated with the final error and for eye movements the correlation is very high, therefore the ccf(1) would be undistinguishable from the acf(1) of either the actual error or action onset. Similarly, a zero cross-correlation ccf(1) would denote an optimal change of the time of action onset to correct for the previous error.

Dependency on the previous actual temporal error

We analyzed the dependency of the time of action onset in the current trial on the temporal error with respect to the target in the previous trial in the different conditions by fitting linear mixed-effect models (LMMs), which enable us to easily analyze the effects of the previous trial on the current response. In the model, the action onset time was the

288 dependent variable and the previous target temporal error, the independent variable. Both
289 intercept and slope were allowed to vary as random effects across subjects Both intercept
290 and slope were allowed to vary as random effects across subjects. We used the lmer
291 function (v.1.0–6) (25) from R software

292 Simulations and process modelling

293 In order to estimate the prediction error relative to action onset we used a Kalman filter to
294 estimate the predicted action onset time before the actual observation. For the Kalman
295 filter to work, one needs knowledge of the sources of variability (process and measurement
296 noise). To get further insight into the variance of the generative process of the action onset,
297 we implemented the temporal corrections at the action onset across simulated trials in
298 which we manipulated different sources of variability: process variability and
299 measurement (i.e. motor) variability. The process variance in the time of action onset is
300 captured by the following expression and mainly accounts for variability of sensory origin:

301 $$V_t = \left(\frac{\sigma_x}{v}\right)^2 + \sigma_t^2 \qquad (1)$$

302 The first term is velocity dependent and the second one corresponds to a timing variability
303 (26). σ_x is the spatial variability about the target position at action onset and v is the target
304 speed. Uncertainty caused by measuring target speed may likely contribute to the timing or
305 velocity dependent variability. However, in practice both sources of variability are difficult
306 to tease apart because an error in misjudging the target position would be
307 indistinguishable from a timing error. In each simulated trial i the generation of an

intended action onset τ is a stochastic process where τ_i, the planned action onset at trial i, is updated according to:

$$\tau_{i+1} = \tau_i - \beta e_i + q, \quad q \sim N(0, V_t) \qquad (2)$$

where β is a learning rate or, in our case, the simulated fraction of error (e) correction and q is the process noise related to eq. 1. The actual action onset T^s is simulated by adding measurement noise (produced by motor noise) to the intended action onset:

$$T_i^s = \tau_i + r, \quad r \sim N(0, \sigma_m^2) \qquad (3)$$

where r is the execution noise (added noise from when the motor command is issued until movement onset). The final temporal error e at trial i is given by:

$$e_i = T^T - (T_i^s + T_i^m) \qquad (4)$$

where T^T is the time at which the target is centred within the interception zone and T_i^m is the movement time. Without loss of generality, we set T_i^m and T^T to zero.

Modeling the corrections. Using the equations introduced above, we modeled a trial-to-trial correction of the time of initiation, assuming that all the final temporal error is fully caused by the time of action initiation T^s. This was certainly the case in the eye movement conditions and button press conditions – because in our case the time to reach the target was fixed once the button was triggered - while for arm movements there is some room for online corrections by adjusting the movement time. We modeled 16 different correction fractions from 0.06 to 1 by increments of 0.06 (range: 0.06-0.96) and four values of r ($\sigma_m =$ 0.022, 0.05 0.1 and 0.2 s). We set σ_x to 1 cm and σ_t to 0.05 s. These values were used with three target velocities: 20, 25 and 30 m/s resulting in a mean process noise variance of

0.0042 s^2. These choices were guided by values reported in previous studies (26,27). If the simulated time at trial *i* was shorter (i.e responding too early) than a target value (e.g. 0 ms) by some magnitude e_i, the value of the intended time onset (τ_{i+1}) was increased by βe on the next trial, or decreased if the observed time was too long. We ran 1000 simulations for each combination of β and *r*. Each simulation consisted of a series of 360 responses or trials in which speed was interleaved (but note that the time the target took to reach the interception zone was the same for all speeds, so target speed changes between consecutive trials are not a problem for making trial-by-trial corrections).

Estimation of process and measurement variances

The fraction of correction β can be estimated from the behavioural data through the Kalman gain (K) (9). The Kalman filter estimates the planned action onset as the hidden state from the actual (noisy) action onsets. In order to know K one possibility is to estimate the process (V_t) and measurement (σ_m^2) variances (28). In steady state (which in our experiments was approached after a few trials), K can be approximated by the following expression (5):

$$K = \frac{V_t}{V_t + \sigma_m^2} \qquad (5)$$

Since V_t and σ_m^2 are known in the simulations, this expression approximates the corresponding optimal correction fractions for the different values of simulated motor (measurement) noise: K= 0.09, 0.29, 0.61 and 0.86 starting with largest value of σ_m^2.

This is not as straightforward when analyzing the behavioral data since both parameters are unknown. In order to estimate the process noise variance V_t in the different experimental conditions, we proceeded as follows: first we fitted a linear model to the process noise variance in the simulated data based on terms that could be obtained from the observed data (both simulated and behavioral). Second, we used the fitted model to predict the process variance in the experiments.

The linear model contained three terms plus their interactions. Two of the terms come from the decomposition of the actual temporal variance into estimates of $(\sigma_x/v)^2$ and σ_t^2 which may contain measurement noise because they were estimated from the observed simulated data. The third term was the ccf(1) of the action onsets. When we fitted the model to the process noise variance in the simulated data the model accounted for the 94% of the variance.

In order to obtain the two first terms of the linear model in both simulated and behavioral data, we fitted the following model (29) to the total spatial variability:

$$SD_x = \sqrt{\sigma_x^2 + (v\sigma_t)^2} \qquad (6)$$

We estimated σ_x and σ_t^2 for each series of 360 trials in the simulations and for each participant and condition. Fig S1A shows the simulated process variance against the predicted process variance from the model. Fig S1B shows the estimated process variance in the human data based on the linear model used to fit the process variance in the simulated data. The process variance is plotted against the whole observed temporal variance. Fig S1C shows how the whole temporal variance is decomposed according to equation eq. 1.

Once we had estimated the process variance V_t, the measurement noise was the only free parameter when fitting the Kalman filter to the behavioral data.

The Kalman filter model

We applied a Kalman filter model to determine the degree of correction based on the prediction error. As shown in eq. 3 the actual action onset T^s is a noisy realization of the predicted action onset τ. We can rewrite eq. 2 as:

$$\tau_i = \tau_{i-1} + c_i + q \qquad (7)$$

where c_i is a correction factor that has to be determined by the Kalman filter. But, how does the Kalman filter work out the magnitude of the correction? The Kalman estimates c_i recursively by combining a predicted action onset (i.e. a priori) and the observation of action onset that has been corrupted by noise T^s. After movement onset at trial *i*, the Kalman filter estimates a posterior time of action onset (denoted by the hat operator):

$$\hat{\tau}_i = \tau_i + K_i(T_i^s - \tau_i) \qquad (8)$$

The posterior will be used as a predicted action onset time in trial *i+1*, becoming τ_i in (eq. 7). K_i is called the Kalman gain and reflects the fraction of correction of the prior time of action onset. If $K = 0$ no change is made in the planning for the next trial; alternatively, if $K = 1$ the whole difference between the prediction and the observed action onset is accounted for in the posterior. We will refer to the difference between T^s and τ as *prediction error*.

In order to compute K, the Kalman filter takes into account the uncertainty of the prediction and the one of the observation.

$$K_i = P_i(P_i + \sigma_m^2)^{-1} \qquad (9)$$

where P_i is the uncertainty in the prediction of the planned onset time before the observation of action onset takes place. Note the equivalence with eq. 5. This *a priori* uncertainty is also obtained from the posterior estimate of the uncertainty, $\hat{P}$, in trial *i-1*:

$$P_i = \hat{P}_{i-1} + V_t \qquad (10)$$

The Kalman filter will correct the internal estimate (i.e. predicted action onset) by a fraction K of the prediction error $T^s - \tau$. However, although the prediction error is highly correlated with the final temporal target error in some conditions, the prediction error is not the task-relevant error shown in eq. 4. We analysed the correction with respect to action onset because we are interested in how people correct in the planning phase.

The planning of the action onset should aim at minimizing the expected final temporal error ($e(\tau) = 0$) which can be stated as:

$$e = T^T - \tau + T^m \qquad (11)$$

In order to be accurate across all observed responses we need that:

$$T^T = T^s - T^m \qquad (12)$$

Substituting eq. 12 in eq. 11:

$$e = (T^s - T^m) - (\tau + T^m) = T^s - \tau \qquad (13)$$

which is the prediction error with respect to action onset that the Kalman filter is correcting. This equation shows that, given some constraints in the distribution of movement time T^m (i.e. shifted mean with respect to T^s), correcting for the prediction error is equivalent to correcting for the final temporal error. This is true on average, since for individual trials the prediction error does not necessarily correspond to the final error.

Parameter estimation. In order to estimate the predicted action onset time (τ) σ_t^2, the measurement noise was the only free parameter. σ_t^2 was determined by minimizing the negative log-likelihood of the actual action onset given the estimated (planned) action onset computed by the Kalman filter in each participant and condition.

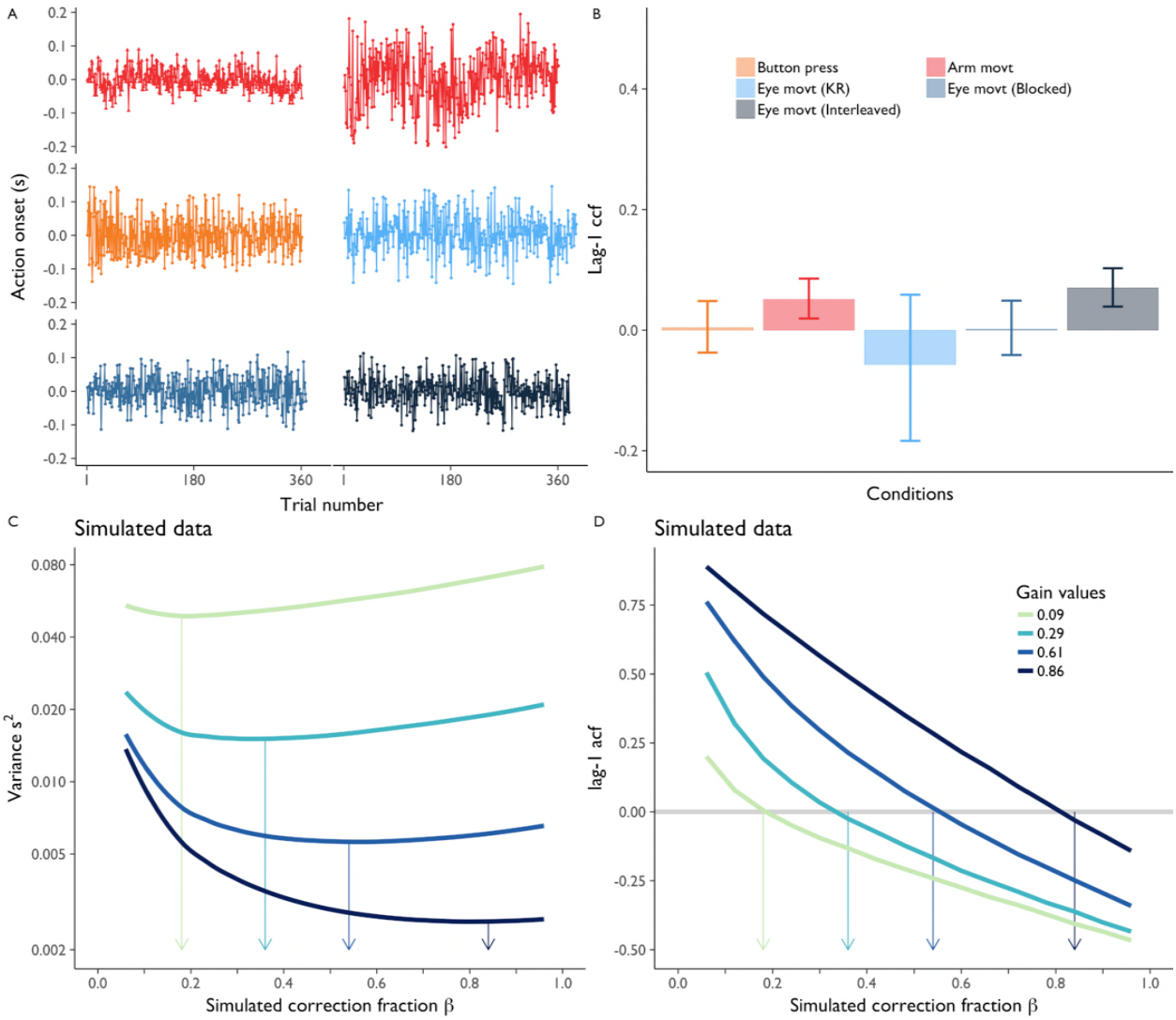

417

418 *Fig 2. (A) Example of action onset times for the different conditions. Different conditions are*
419 *color-coded (see legend in Fig2B). Each response series corresponds to a single participant.*
420 *The two examples of the arm movement condition correspond to a fast (top-left) and slow*
421 *(top-right) participant. The action onset time is centered at zero (by substracting the mean)*
422 *to optimize panel space. (B) Mean lag-1 cross-correlation functions, ccf(1), between the time*
423 *of action onset at trial t and actual temporal error at trial t-1 for the different conditions.*
424 *Error bars denote the 95%-CI of the correlation coefficients. (C) (Simulated data) The*
425 *temporal error variance as a function of the simulated fraction of correction β for the four*
426 *different levels of simulated execution noise. The arrows point to the value of β that*
427 *corresponds to the minimum variance. As can be noted, this fraction of correction is similar to*

the simulated gain (which in turn depends on the level of execution noise, see legend in panel D). The largest gain (i.e. K=0.86) requires larger corrections in order to minimize the variance. (D) (Simulated data) The acf(1) values of action onset in the simulated data against the amount of correction. As can be seen, the acf(1) should be near zero to be optimal for each gain.

Results

Are temporal corrections optimal?

Assuming that open-loop control schemes are used to execute the movements, we expect a modulation of the initiation times by prior temporal errors but also that the time of action initiation relative to the interception time is not statistically different across different target velocities. That is, relevant decision variables regarding the action onset would mainly rely on temporal estimates of the remaining time to contact from the action initiation. An ANOVA on the linear mixed model in which action onset was the dependent variable, target speed (fixed effect as continuous variable), conditions (fixed effect as factor) and subjects treated as random effects failed to report a significant effect of target speed on action onset ($F<1$, $p=0.96$) and only condition was significant ($F=53$, $p<0.001$). The interaction was not significant ($F<1$, $p=0.473$).

Fig 2A shows examples of series of observed action onset times from the different experimental conditions. From the different series we first computed the lag-1 cross-correlation function (ccf(1)) between the action onset in trial t and the temporal error in trial t-1. To qualify as "optimal correction", ccf(1) between previous target error and action onset must be zero (or very close to zero). Fig 2B shows the mean lag-1 cross-correlation

function ccf(1) between the time of action onset and previous error for the different conditions. These values are consistent with participants changing their action onset optimally or near optimally. ccf(1) values for arm movements and eye movements (KP-interleaved) were very low but significantly different from zero.

We conducted the same analysis on the simulated data. First, Fig 2C shows how the fraction of correction modulates the overall temporal variance. The correction fraction for which the temporal variance is minimal is the optimal correction fraction. This fraction is different for the different levels of simulated execution or motor noise (measurement noise) that correspond to the different Kalman gains. Importantly the values of optimal correction correspond to values of ccf(1) (or acf(1) in the simulations) very close to zero (Fig 2D). From the different data patterns shown in Fig 2 we can be quite confident that participants corrected by changing the time of action onset in an optimal way or close to an optimal way.

Dependency on the previous temporal error

Autocorrelation indicates how consecutive points tend to be around the mean (e.g. if one overcorrects then consecutive points will likely be on opposite sides), but does not indicate which fraction of the previous actual error is being accounted for in the change of action onset in the present response. In order to get an estimate of this magnitude we ran the Linear Mixed Model (described in the methods sections). The time of action initiation at each trial was fitted as a function of the previous final temporal error. The slope denotes how much the previous error is considered. Fig 3A (red dots for the Arm movement condition and boxplot) shows the values of the slopes. The larger slopes were found in the

arm movement condition and the average slope was significantly different from zero (slope=0.12 fraction/trial, t=5.39, p<0.0001). For the remaining conditions, only in the Eye movements (KP-interleaved) the slope was significantly different from zero (slope=0.07 fraction/trial, t=3.78, p=0.004). The distribution of individual slopes in the Arm movements condition reveals an interesting and clear positive linear relation between the movement time and the dependency on the previous temporal error (Fig 2A main panel). Participants with slower arm movements modified more the action onset in the present trial more as a function of the previous interception temporal error. Movement time in saccades did not have enough variability across subjects to observe a similar distribution and cursor movement time was fixed in the button press condition. The corrections in the Button press and Eye movements conditions (KR and KP-blocked) did not rely on the previous temporal error with respect to the target (slopes not different from zero).

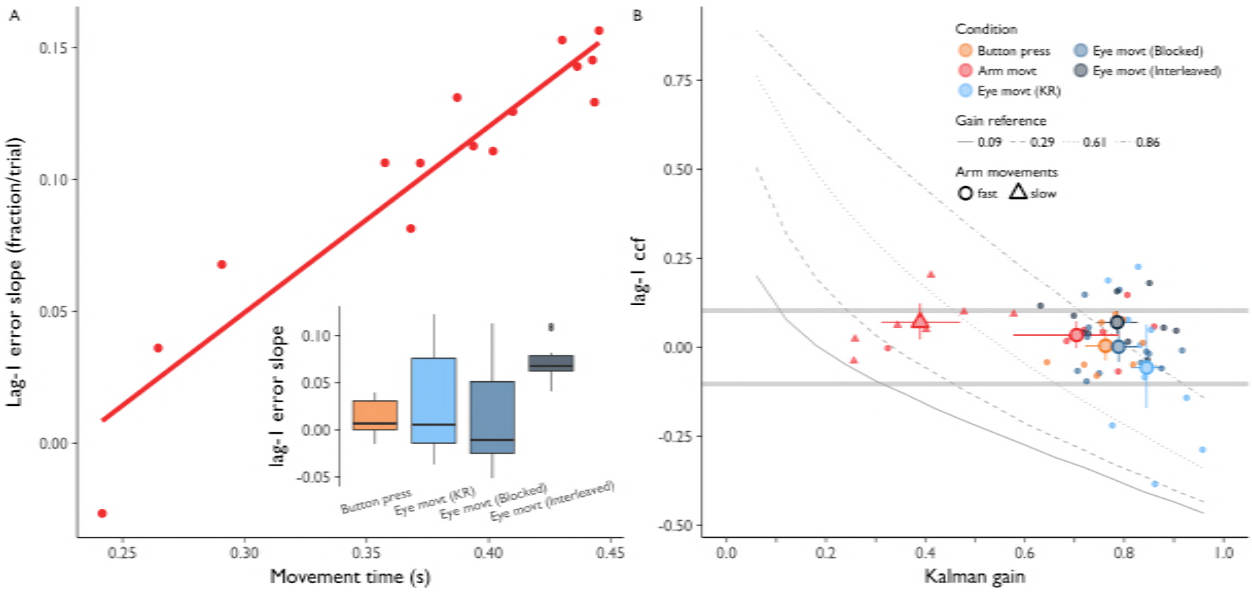

Fig 3. (A) Dependency (slope in the linear model) of the action onset on the previous actual temporal error as a function of movement time in the Arm movement condition. Each dot corresponds to an individual participant. (inset) The slopes (boxplot) corresponding to the

other conditions. (B) The ccf(1) for each participant against the estimated Kalman gain (K). Smaller dots correspond to individual participants and conditions, while larger dots are mean values across subjects within conditions. For the Arm movement condition we split the data points into slow and fast participants depending on the movement time (shape coded). Error bars denote 95%-CI. The two horizontal grey lines denote the confidence interval for the null ccf. For the sake of coparison, the four lines with different styles (dolid, dashed, dotted and dash-dotted) correspond to the Kalman gain and expected ccf obtained in the simulations (see Fig 2D).

The question then is how do people correct in these conditions? One possibility (depicted in Fig 1A) is that people corrected the aimed action onset, not based on the final temporal error but on the difference between the planned action onset and the actual action onset (i.e. the prediction error). Since we could not measure this prediction error in the experiment, we had to model correcting based on this error to infer how large these corrections were. We used a Kalman filter model to estimate the Kalman gain, that is the fraction of the prediction error that is used to update the aimed action onset for the next trial.

Corrections based on the action onset prediction error

Unlike in the simulations, both the process (V_t) and measurement (σ_m^2) variances are unknown in the experiments. The Kalman filter requires knowledge of these variances in order to estimate the optimal Kalman gain (K). We inferred the process noise variance (V_t) in the experimental data by predicting this variability from the linear model that was used to fit the process noise variance in the simulations.

The standard deviation of the process noise for the eye movements (KR) was larger than in the other conditions (58 ms versus 37 ms in Button press, 38 ms in Arm movements, 44 ms in Eye movements KP-Blocked and KP-interleaved). Only the difference between KR and Arm movements reached significance (corrected p=0.009). For the hand movements condition, we found a clear difference between slower and faster (<400 ms of movement time) participants with the latter being more variable (49 ms versus 17 ms, p<0.0001).

The Kalman filter was fitted to the time series based on the action onset with the measurement noise variance (σ_m^2) as the only free parameter.

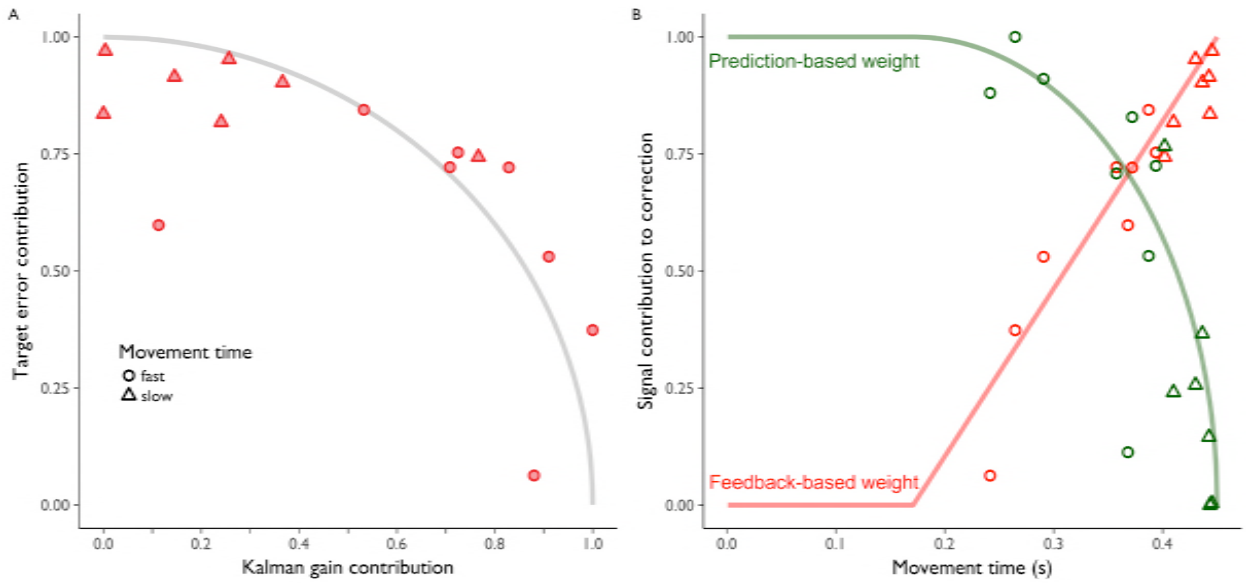

Fig 4. (A) Relation between the contribution to the correction of the action onset based on the previous temporal error (Target error contribution) and the contribution to the correction based on the prediction error (i.e. based on the Kalman gain) for the Arm movement condition. Each dot corresponds to a different participant and the shape corresponds to the classification of the movement time duration (fast: less than 0.5 s; slow larger than 0.5 s). The target error contribution between 0 and 1 corresponds to the actual fraction of correction of the final error obtained from the slopes shown in Fig 3A by using a linear the model. The linear model was obtained with the simulated data and allowed to estimate the

corresponding slope for each (simulated) fractions of corrections. The Kalman gain contribution is obtained by scaling the Kalman gain between 0 and 1. The grey line corresponds to the predicted relation assuming that both correction fractions are combined into a quadratic sum (equation 14) (B). Evolution in time of the correction fractions (i.e. relevance given to prediction and final error). The shift of the two lines (prediction and feedback-based correction) depends only on the time at which the final temporal error will start to be considered for correction in the next trial (about 171 ms in the figure). See text and equation 15 for the computation of the two lines in panel B.

The individual as well as the mean Kalman gains for participants and conditions are shown in Fig 3B together with the value of the ccf(1). This plot shows that different values of correction with respect to the action onset prediction error (i.e. Kalman gain) can correspond to optimal or near optimal corrections. The estimated magnitude of the measurement noise was very similar among conditions and its standard deviation ranged from 33 ms (Arm movements) to 35 ms (Eye movements KP-Blocked). No difference was significant. There was no difference between slow (31 ms) and fast (34 ms) participants in the arm movement condition. Thus, the differences in process to measurement variance ratio that determines the Kalman gain are due to differences in the process noise. Fig 3B also shows the difference between slow and fast participants in the Arm movement conditions with the parameters corresponding to the fast group being very similar to those of the Eye movements and Button press conditions. This is consistent with people correcting less based on the prediction error (difference between planned action onset and actual action onset) when they moved more slowly.

This high Kalman gain (i.e. use of prediction error) would be expected in the Eye movement conditions because the sensory feedback of the final temporal error can be noisy. However

551 this is not the case for the Button press condition in which participants could perfectly
552 perceive the error. Since the final temporal error is fully explained by the time of action
553 onset in this condition, it seems that the correction based on the prediction error rather
554 than the final error seems to be based on the reliability (or correlation) of the prediction
555 error with respect to the final temporal error.

556 Relation between prediction error and final temporal error

557 Based on the auto-correlations, people make corrections that minimize the temporal
558 variability across trials. However, in some conditions there is no dependency on the
559 previous temporal error. One possibility that would explain this apparent contradiction is
560 that people correct based on some combination of the prediction error and the final
561 temporal error, with this combination being modulated by the movement time. This would
562 explain the difference in Kalman gain between slow and fast movement times in the Arm
563 movement condition. The prediction error (actual onset minus planned onset times) would
564 be weighted more heavily in the next trial for short movement times with a progressively
565 decay in favor of the final temporal error (relative to the target) as movement time
566 increased (Fig. 1A). The estimated Kalman gains support this hypothesis, but to further
567 explore this possible use in combination of both error signals we plotted the relation
568 between the (normalized) dependency on the actual previous temporal error and the
569 Kalman gain contribution (1 meaning that all the estimated Kalman gain is used for
570 correction) for the different subjects who participated in the Arm movements condition
571 (Fig 4A). Interestingly, the relation between the corrections fractions based on both types
572 of errors resembles a specific type of combination described by the grey line in Fig4A. This

line denotes a quadratic sum of the two error signals contributions (x and y axes). For example, if we take any point (x,y) along the grey line (e.g. x=0.7, y=0.72), the quadratic sum $\sqrt{(x^2 + y^2)}$ adds to one.

Faster subjects (circles in Fig 4A) show larger Kalman gains (as in Fig 3B) and the dependency on the previous target error is small. This trade-off changes for slow participants (triangles in Fig 4A). This transition is well described by the grey line that corresponds to a quadratic sum of the two fractions of correction:

$$\omega = (\beta^2 + K^2)^{1/2} \qquad (14)$$

where β and K correspond to the contributions of the actual temporal error and prediction error respectively and ω denotes the trade-off between the two error signals.

Some models of cue combination (30) have used the expression represented by eq. 14 to define the combined reliability (i.e. reciprocal of variance) from the individual reliabilities. In this sense equation eq. 14 captures the maximum likelihood estimation of the combined reliability. Such a combined use of error signals (not contemplated in our model) results in an increased precision with respect to using either signal alone. However, one important assumption is that the individual reliabilities are independent (i.e. uncorrelated). This is not the case in our two temporal error signals. The prediction error and the final target error are highly correlated in our conditions (see Fig S2). Due to the magnitude of the correlation, there is very little or no benefit in correcting based on integrating or combining both error signals (31) (see Fig S3). The expression in eq. 14 then should not be interpreted as a weighted combination but as denoting the trade-off between the two error signals.

Fig 4A does not contain any temporal information concerning how the relevance of each signal β and K evolves over time. The modulation of the relative relevance in next trial by the movement time (Fig. 4B) sheds some light on how both types of errors (the prediction error based on K and the final temporal error based on β) evolve over time. Fig 4B simply plots the same points shown in Fig 4A as a function of the corresponding movement time for each point. As can be seen, the relevance of the prediction error decreases in a non-linear manner, while the contribution of the target error increases linearly. Moreover, Fig 4B shows that the increase of β takes place after some critical movement time or sensorimotor delay δ_{sm}. We can formulate this trend (red lines in Fig 4B) according to the following piecewise function:

$$\beta_t = \begin{cases} 0, & \text{if } T^m \leq \delta_{sm} \\ aT^m, & \text{otherwise} \end{cases} \qquad (15)$$

where T^m is the movement time. On the other hand, we can obtain how the corresponding fraction of correction given to prediction (K) as a function of the change in β across time from eq. 14. The value of K is expected to decrease with time according to this expression (green line in Fig 4B):

$$K_t = (1 - \beta_t^2)^{(1/2)} \qquad (16)$$

We only adjusted δ_{sm} in Fig 4B so that the dcrease of K_t and simultaneous increase of β_t minimized squared errors across the red and green dots in Fig 4B. The parameter a in eq. 15 will then depend on δ_{sm}. In our case a=3.58. The obtained value of δ_{sm} was 170 ms. This value imposes a lower temporal bound on the movement time from which the final temporal error with respect to the target will be considered to be corrected for in next trial.

Discussion

We show that people minimize the temporal variance across trials when correcting for temporal errors. This is concluded from the structure of temporal correlations (32): we report near zero lag-1 ccf between action onset and the previous temporal error in an interception task. However, which error signal is predominantly used to correct differs depending on the condition and duration of the movement of the action: slower movements showed larger dependency on the previous final temporal error with respect to the target in the Arm movement condition. In most conditions (Eye movements, Button press and fast Arm movements), people strongly rely on the prediction error at action onset rather than the actual temporal error with respect to the target to change the planned initiation time in the next trial. This is based on the high values of the Kalman gain, which denotes that the prior (planned) action onset will be shifted in the next trial by a large fraction (about 0.8) of the prediction error (i.e. difference between the prior and actual action onset). In the Arm movements condition, fast movements were initiated later, therefore their planning could have been more robust than slow movements (initiated earlier) increasing the reliability of the prediction error. The reliance on the prediction error has obvious advantages when the final sensory feedback is noisy. This is the case in the Eye movements conditions where perception of the sensory temporal error signal can be noisy. Correcting from the prediction error at action onset is possible under some restrictions (e.g. open loop), as there is a clear correlation between the prediction error and the final temporal error (Fig S2). Due to the possibility of making corrections during

636 the movement, the correlation is lower in the Arm movement condition, and this is the
637 condition in which we find less contribution of the prediction error (slower movements).

638 Models of motor learning would predict less correction (e.g. lower learning rate) when the
639 sensory feedback is more uncertain (5,10,11,9) or if error signals are perceived less
640 relevant (7,33). The Bayesian explanation is that the sensory error feedback is weighted
641 less in favor of internal state estimates (34). This is usually the case when studies focus on
642 the reliability of the final task-relevant error. Our findings, however, show that the picture
643 can be more complex. We found the same amount of correction in the Eye movements and
644 Button press conditions while the final temporal error signal is likely perceived with very
645 different uncertainty, as the Button press is more reliable. Our results show that
646 corrections in these two conditions are executed in a very similar way (similar Kalman
647 gains and dependency on the previous temporal error). The way temporal errors are
648 corrected (mainly in the Button press condition) challenges some of the assumption of
649 current models, and merely considering the final sensory error might not suffice, at least
650 when temporal errors are relevant. The control at the time of the button press seems to be
651 an important factor as to which error signal will be used to correct in the next trial.

652 Prediction errors have been mostly regarded as relevant for online corrections when the
653 final sensory feedback would arrive too late to make useful corrections. Here we show that
654 prediction errors can be useful for trial-by-trial corrections after the actual error is known.
655 This process is apparently not affected by low uncertainty of the final error (e.g. Button
656 press condition) because it does not override the use of the prediction error at action onset.
657 Interestingly, it seems that the contribution of the final error for next trial correction

658 depends on the movement time. We found that the final target error will start to be
659 weighted for correction in the next trial by movement times close to 200 ms. This is
660 consistent with the value that has recently been reported for online spatial corrections
661 when there is a target movement (35). The model (Fig 4B) also predicts that, as movement
662 progresses, the reliability of the prediction error at action onset decreases reaching a
663 minimum after 400 ms. This time course of the contribution of the prediction error for the
664 next trial parallels the shift from prediction to sensory signals in online correction of
665 spatial errors of arm movements (12).

666 The evolution of the contirbution given to prediction and final errors suggests that the
667 system has some access to or knowledge about the noise that is added from the time of
668 action onset. This would be in agreement with previous work showing that the motor
669 system is able to model the temporal uncertainty of the movement time when
670 programming reaching movements under temporal constraints (36).

671 The relevance of the prediction error in trial-to-trial temporal corrections is mostly
672 noticeable in the Eye movements condition. The behavioral plasticity of the saccadic
673 system has been well established in the temporal domain: saccade latencies may be
674 strongly affected by a number of factors such as temporal stimulus arrangement (37),
675 stimulus properties (38,39), urgency (40), expectations (41) or reinforcement
676 contingencies (42). Moreover, studying saccades directed toward a moving target revealed
677 that the saccadic system takes into account both the saccade latency and duration, and is
678 able to adjust to experimentally induced perturbations (43). Our current results shed a new
679 light on the underlying adaptive process revealing that the temporal error is integrated on

680 a trial-to-trial basis to adjust the saccade-triggering. It is noteworthy that these conclusions
681 nicely echoe ones from saccade adaptation studies in which the adjustment of saccade
682 amplitude has been well accounted for by postulating a Bayesian integration in which the
683 weight associated with each piece of information is adjusted depending on the sensory
684 evidence available (2).

685 Concerning the eye movements, we found a small but significant dependency of the final
686 temporal error on whether the target speed was interleaved and knowledge of
687 performance based on the final error was provided (KP-interleaved). Although the
688 correlation between the final temporal error and prediction error is slightly weaker in the
689 interleaved condition (slope of 0.75 Fig S2) than in the other two Eye movements
690 conditions (slope of 0.80 and 0.81), the differences are not significant. The Kalman gain was
691 not significantly smaller in this condition (KP-interleaved) compared to when the speed
692 was blocked (KP-Blocked), which denotes also a strong weight of the prediction error.
693 However, the condition of a non-stationary environment (variable speed across trials)
694 could have encouraged a larger contribution of the final error. Note that knowledge of the
695 magnitude of the error was not provided in the KR condition in which the speed was also
696 interleaved. Conditions of stationary environment can be an important factor that also
697 contributes to how the final error is weighted. In addition to stationary stimuli conditions,
698 the temporal restrictions on which feedback is provided can also change. One limitation of
699 our study is that we have used a relatively constant temporal window for participants to hit
700 the moving target and the feedback was given with respect to a fixed temporal window.
701 The learning rates or correction fractions might be also tuned to this temporal requirement
702 and different learning rates could have been observed by varying the temporal window on

703 which feedback was provided. For example, lax temporal constraints would lead to smaller
704 learning rates. Recent studies have shown that different sensitivities to execution errors
705 arise in motor learning depending on the stationary conditions of the environment (44).
706 From our study we do not know whether the specific weighting pattern of the two signals
707 can be generalized to other conditions, such as non-stationary environments in which the
708 temporal constraints are not constant. Future studies will have to address whether flexible
709 learning rates also apply to the temporal domain.

710 Acknowledgements

711 We thank Cristina de la Malla for providing feedback on an earlier version of the
712 manuscript. This project was supported by Grants PSI2017-83493-R from MINECO and
713 2017SGR48 from the Catalan government and PACE H2020-MSCA-ITN-2014 Ref. 642961.

714 References

715 1. Pearce JM, Hall G. A model for pavlovian learning: Variations in the effectiveness of
716 conditioned but not of unconditioned stimuli. Psychological review. 1980;87(6):532.

717 2. Shadmehr R, Smith MA, Krakauer JW. Error correction, sensory prediction, and
718 adaptation in motor control. Annu Rev Neurosci. 2010;33:89–108.

719 3. Thoroughman KA, Shadmehr R. Learning of action through adaptive combination of
720 motor primitives. Nature. 2000;407(6805):742–7.

721 4. Donchin O, Francis JT, Shadmehr R. Quantifying generalization from trial-by-trial
722 behavior of adaptive systems that learn with basis functions: Theory and experiments in
723 human motor control. J Neurosci. 2003 Oct;23(27):9032–45.

724 5. Burge J, Ernst M, Banks MS. The statistical determinants of adaptation rate in human
725 reaching. J Vis. 2008;8(4):20.1–19.

726 6. de la Malla C, López-Moliner J, Brenner E. Dealing with delays does not transfer across
727 sensorimotor tasks. J Vis. 2014;14(12).

728 7. Herzfeld DJ, Vaswani PA, Marko MK, Shadmehr R. A memory of errors in sensorimotor
729 learning. Science. 2014 Sep;345(6202):1349–53.

730 8. van Beers RJ. Motor learning is optimally tuned to the properties of motor noise. Neuron.
731 2009;63(3):406–17.

9. van Beers RJ. How does our motor system determine its learning rate? PloS one. 2012;7(11):e49373.

10. Kording KP, Tenenbaum JB, Shadmehr R. The dynamics of memory as a consequence of optimal adaptation to a changing body. Nature neuroscience. 2007;10(6):779.

11. Wei K, Körding K. Uncertainty of feedback and state estimation determines the speed of motor adaptation. Frontiers in computational neuroscience. 2010;4.

12. Wolpert DM, Ghahramani Z, Jordan MI. An internal model for sensorimotor integration. Science. 1995;269(5232):1880–2.

13. Desmurget, Grafton. Forward modeling allows feedback control for fast reaching movements. Trends Cogn Sci. 2000 Nov;4(11):423–31.

14. Shadmehr R, Krakauer JW. A computational neuroanatomy for motor control. Exp Brain Res. 2008 Mar;185(3):359–81.

15. Xu-Wilson M, Chen-Harris H, Zee DS, Shadmehr R. Cerebellar contributions to adaptive control of saccades in humans. Journal of Neuroscience. 2009;29(41):12930–9.

16. Mazzoni P, Krakauer JW. An implicit plan overrides an explicit strategy during visuomotor adaptation. J Neurosci. 2006 Apr;26(14):3642–5.

17. Taylor JA, Ivry RB. Flexible cognitive strategies during motor learning. PLoS computational biology. 2011 Mar;7(3):e1001096.

18. Diedrichsen J, Hashambhoy Y, Rane T, Shadmehr R. Neural correlates of reach errors. J Neurosci. 2005 Oct;25(43):9919–31.

19. Binda P, Cicchini GM, Burr DC, Morrone MC. Spatiotemporal distortions of visual perception at the time of saccades. Journal of Neuroscience. 2009;29(42):13147–57.

20. Bremmer F, Kubischik M, Hoffmann K-P, Krekelberg B. Neural dynamics of saccadic suppression. Journal of Neuroscience. 2009;29(40):12374–83.

21. Teasdale N, Bard C, Fleury M, Young DE, Proteau L. Determining movement onsets from temporal series. Journal of motor behavior. 1993;25(2):97–106.

22. Brainard DH. The psychophysics toolbox. Spatial vision. 1997;10:433–6.

23. Pelli DG. The videotoolbox software for visual psychophysics: Transforming numbers into movies. Spatial vision. 1997;10(4):437–42.

24. van Beers RJ, Brenner E, Smeets JBJ. Random walk of motor planning in task-irrelevant dimensions. J Neurophysiol. 2013;109(4):969–77.

25. Bates D, Maechler M, Bolker B, Walker S. Fitting linear mixed-effects models using lme4. Journal of Statistical Software. 2015;67:1:48.

765 26. Brenner E, Smeets JBJ. Sources of variability in interceptive movements. Exp Brain Res.
766 2009;195(1):117–33.

767 27. López-Moliner J, Supèr H, Keil M. The time course of estimating time-to-contact:
768 Switching between sources of information. Vision Res. 2013;92:53–8.

769 28. Mehra R. On the identification of variances and adaptive kalman filtering. IEEE
770 Transactions on automatic control. 1970;15(2):175–84.

771 29. Linares D, Holcombe AO, White AL. Where is the moving object now? Judgments of
772 instantaneous position show poor temporal precision (sd = 70 ms). J Vis. 2009;9(13):9.1–
773 14.

774 30. Ernst MO, Banks MS. Humans integrate visual and haptic information in a statistically
775 optimal fashion. Nature. 2002;415:429–33.

776 31. Oruç I, Maloney LT, Landy MS. Weighted linear cue combination with possibly
777 correlated error. Vision research. 2003;43(23):2451–68.

778 32. van Beers RJ, Meer Y van der, Veerman RM. What autocorrelation tells us about motor
779 variability: Insights from dart throwing. PLoS One. 2013;8(5):e64332.

780 33. Wei K, Körding K. Relevance of error: What drives motor adaptation? Journal of
781 neurophysiology. 2009;101(2):655–64.

782 34. Kording K. Decision theory: What "should" the nervous system do? Science. 2007
783 Oct;318(5850):606–10.

784 35. Franklin DW, Reichenbach A, Franklin S, Diedrichsen J. Temporal evolution of spatial
785 computations for visuomotor control. Journal of Neuroscience. 2016;36(8):2329–41.

786 36. Hudson TE, Maloney LT, Landy MS. Optimal compensation for temporal uncertainty in
787 movement planning. PLoS Comput Biol. 2008 Jul;4(7):e1000130.

788 37. Kalesnykas R, Hallett P. The differentiation of visually guided and anticipatory saccades
789 in gap and overlap paradigms. Experimental Brain Research. 1987;68(1):115–21.

790 38. Madelain L, Krauzlis RJ, Wallman J. Spatial deployment of attention influences both
791 saccadic and pursuit tracking. Vision research. 2005;45(20):2685–703.

792 39. Harwood MR, Madelain L, Krauzlis RJ, Wallman J. The spatial scale of attention strongly
793 modulates saccade latencies. Journal of neurophysiology. 2008;99(4):1743–57.

794 40. Montagnini A, Chelazzi L. The urgency to look: Prompt saccades to the benefit of
795 perception. Vision research. 2005;45(27):3391–401.

796 41. Anderson AJ, Carpenter RHS. Changes in expectation consequent on experience,
797 modeled by a simple, forgetful neural circuit. Journal of Vision. 2006;6:822–35.

42. Vullings C, Madelain L. Control of saccadic latency in a dynamic environment: Allocation of saccades in time follows the matching law. Journal of neurophysiology. 2017;jn–00634.

43. Fleuriet J, Goffart L. Saccadic interception of a moving visual target after a spatiotemporal perturbation. J Neurosci. 2012 Jan;32(2):452–61.

44. Herzfeld DJ, Shadmehr R. Motor variability is not noise, but grist for the learning mill. Nat Neurosci. 2014 Feb;17(2):149–50.

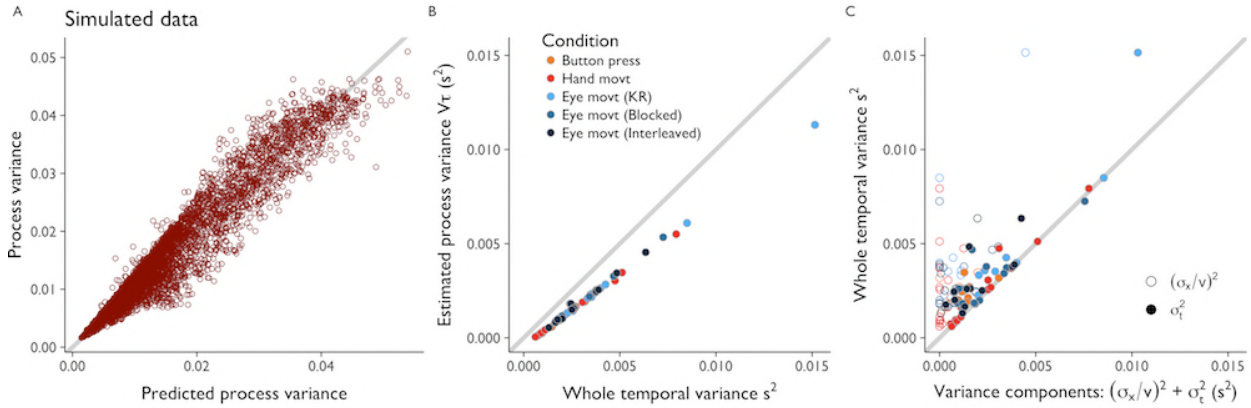

Fig S1. (A) The simulated process variance is plotted as a function of the prediction made from the linear model based on σ_t^2, $(\sigma_x/v)^2$ and the ccf(1). (B) The predicted process variance obtained from the linear model based on the simulated data as a function of the whole temporal variance in the different experimental conditions. (C) Decomposition of the whole temporal variance into the two factors of eq. 1. One can see the part of the variability that comes from spatial (σ_t^2) and temporal ($(\sigma_x/v)^2$) origin.

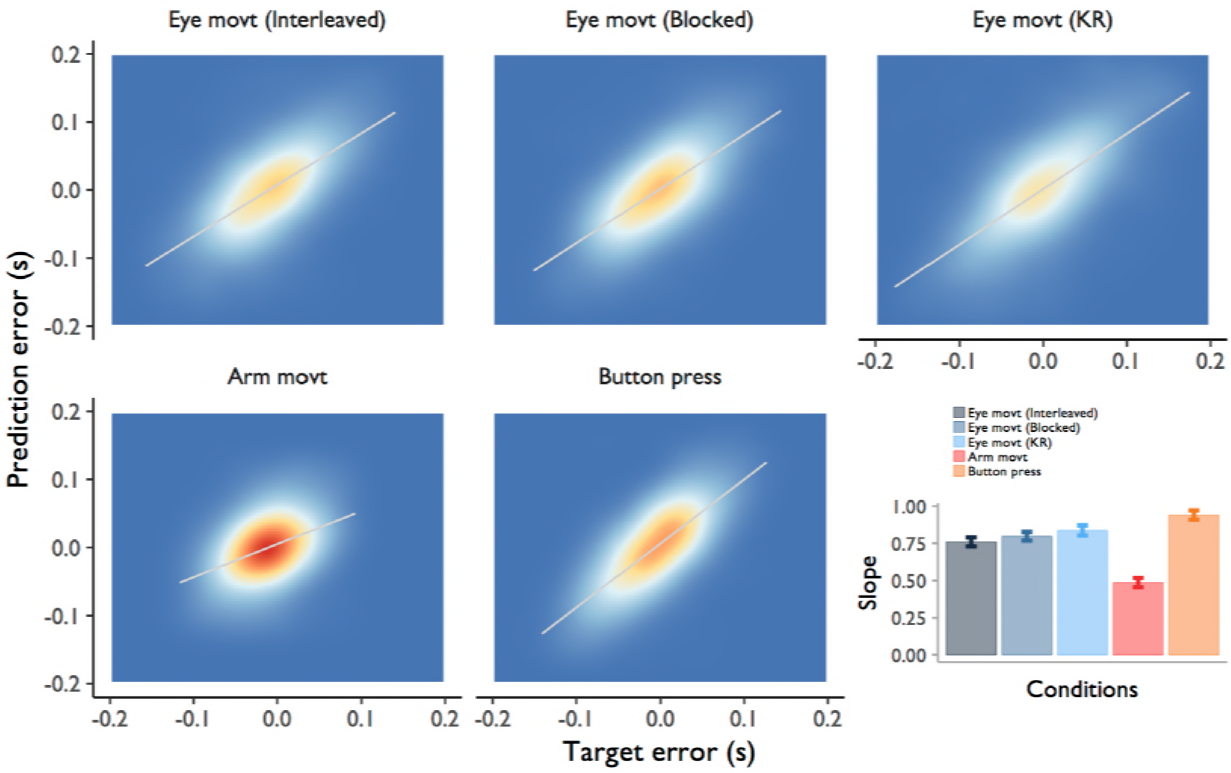

Fig S2. Density between the final temporal error (x-axis) and prediction error (y-axis) that is computed from the Kalman filter for each condition. The density plot includes all participants. The bar plot shows the slope of the fitted (grey) line for each condition. The slope for the Arm movement condition is shown without separating fast and slow movement time. However the slope was significantly smaller for slower movements (0.49 versus 0.72, p=0.01.)

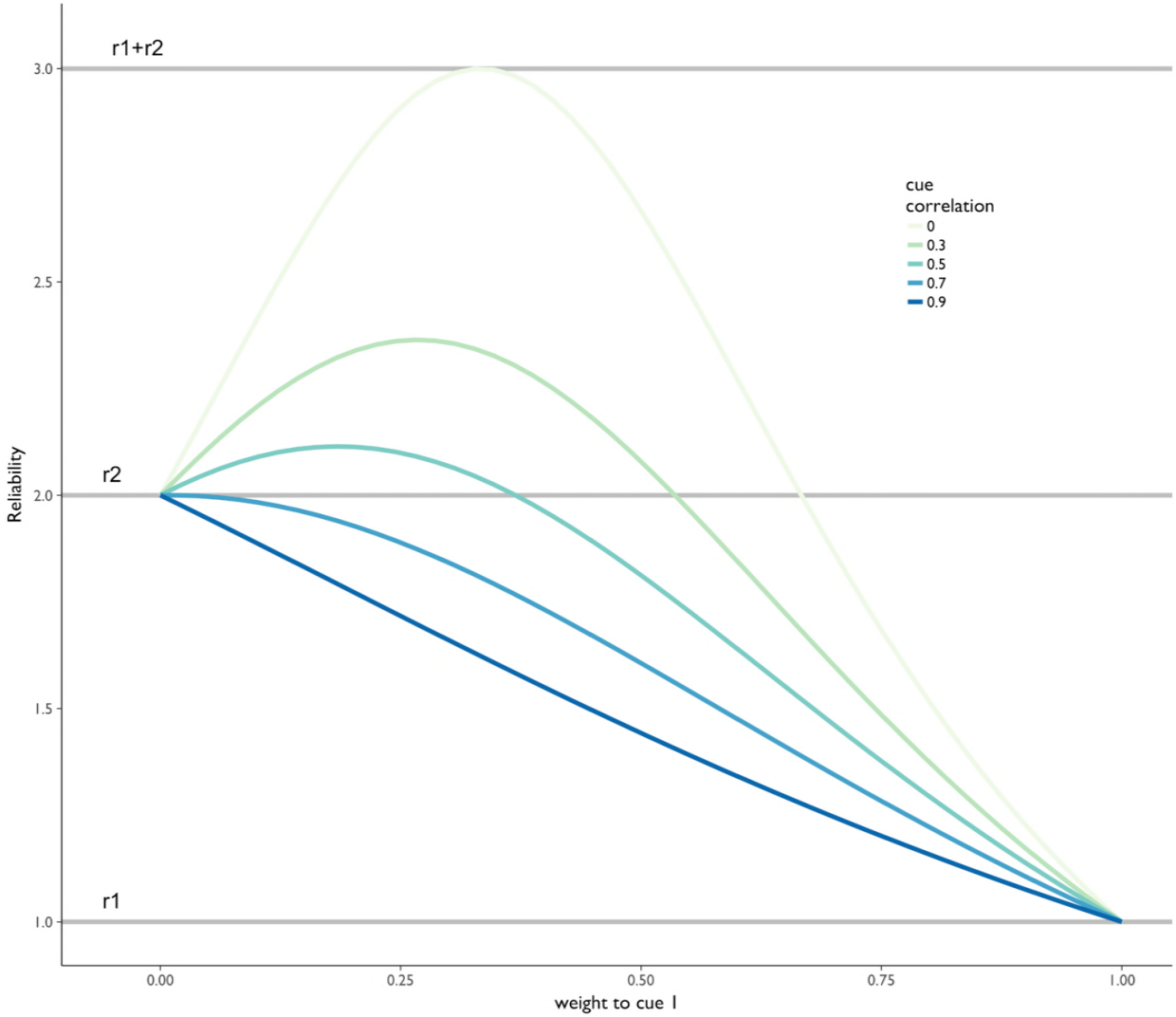

Fig S3. Expected reliability of a weighted linear combination of two cues c1 and c2 with simulated reliabilities r1=1 and r2=2. See (31) for details about the computation of the combined reliability for correlated cues. The x-axis denotes the contribution of cue 1. Five different correlations between c1 and c2 are shown. For the range of correlations observed between the prediction error and the target error (Fig S2) the expected benefit from integration is very little or null.